

**Tricalcium Silicate  $\text{Ca}_3\text{SiO}_5$ , the major component of anhydrous Portland cement: on the conservation of distances and directions and their relationship to the structural elements.**

M.-N. de Noirfontaine <sup>I,II</sup>, F. Dunstetter <sup>I</sup>, M. Courtial <sup>III</sup>, G. Gasecki <sup>II</sup>, M. Signes-Frehel <sup>II</sup>

<sup>I</sup> École Polytechnique, Laboratoire des Solides Irradiés, 91128 Palaiseau, France

<sup>II</sup> Ciments Français-Italcementi Group, C.T.G., rue des Technodes, 78931 Guerville Cedex, France

<sup>III</sup> Laboratoire d'Artois Mécanique et Habitat, Université d'Artois, route de l'Université, 62408 Béthune, France

**Keywords:** alite, cement, orthosilicate, silicate, structure

**Corresponding author:** F. Dunstetter, [mndn@glvt-cnrs.fr](mailto:mndn@glvt-cnrs.fr)

**Abstract.** Tricalcium Silicate, the major component of Portland cement exhibits a complex phase diagram, surprisingly still not completely understood. In this letter, new results are highlighted including a comprehensive study of the superstructure relationship between the polymorphs, and new ideas about the structural analysis. The organisation of the silicate skeleton can be described in terms of 1-D or 2-D elements, from which arise new hypotheses about the cohesion and the chemical origin of the observed superstructures.

## **Introduction**

Tricalcium Silicate ( $C_3S$  within condensed oxide notation) is the major component of anhydrous Portland cement. Seven polymorphs are known, depending on the presence of impurities: T1, T2, T3 (triclinic), M1, M2, M3 (monoclinic) and R (rhombohedral). The conservation of a pseudo-rhombohedral symmetry was first discovered by Jeffery [1] in the monoclinic M3 polymorph. The M1 and M3 forms are most commonly found in the industrial components, but the M1 structure is still unknown. The only known structures are those of the T1, M3 and R polymorphs, investigated by Weisseberg or 4-circle diffractometry (Jeffery [1], Golovastikov et al. [2], Nishi et al. [3,4], Il'Inets [5], Mumme [6]). The aim of our study is to understand the relationships between the known polymorphs, in order to ascertain the structure of the M1 polymorph using powder diffraction data [7].

## **1. Experimental**

Powder samples of triclinic (T1) and monoclinic polymorphs (M1, M2, M3) of Tricalcium Silicate were synthesised in C.T.G. laboratories. X-ray diffraction patterns for each component were collected with a powder diffractometer in Bragg Brentano geometry, with Cu radiation, in the angular range  $10 < 2\theta < 80^\circ$ , with step interval of  $0.02^\circ$  ( $2\theta$ ) and fixed-time counting of 10 s [7].

The data was refined using the Rietveld method [8] and program Fullprof [9] for the T1 and M3 polymorphs, for which atomic models were available, and for M1 polymorph for which a model was determined. All the atomic positions were refined. The silicate tetrahedra were treated as rigid blocks and their orientations were refined. The crystallographic residues  $R_F$  and  $R_B$  were: 13 and 15 for T1 polymorph, 7.8 and 9.1 for M1 polymorph, 14 and 14 for M3 polymorph.

## 2. Constant directions versus superstructure analysis

The M3 polymorph is described in the literature [4] as a 6-fold superstructure (space group Cm) of an  $\langle M \rangle$  elementary block. As can be seen in Table 1 and Fig. 1, it becomes obvious when non-conventional setting of the M3 and  $\langle M \rangle$  unit cells are used. We found polymorph M1 to be also a superstructure of the  $\langle M \rangle$  subcell, but with a different space group (Pc) and 3-fold multiplicity.

No simple relationship was found between the unit cell G determined by Golovastikov et al. [2] for T1 polymorph and the unit cells of the other known polymorphs, except for the conservation of one hexagonal direction:  $\mathbf{b}_G = 2\mathbf{a}_H$ . Here, the H unit cells refer either to the hexagonal unit cell (three times the rhombohedral R unit cell) or to the pseudo-hexagonal unit cells of the monoclinic and triclinic polymorphs. The unit cell vectors of the rhombohedral and monoclinic polymorphs are all located in the two orthogonal hexagonal and monoclinic planes, whereas the two triclinic vectors  $\mathbf{a}_G$  and  $\mathbf{c}_G$  have oblique orientations without any clear relationships with the monoclinic M1, M3,  $\langle M \rangle$  or the hexagonal H unit cells. But one can see that the diagonal  $\mathbf{a}_G + \mathbf{c}_G$  of the triclinic unit cell belongs to the monoclinic plane. Nishi et al. [3] already found such similarity in the arrangement of the atoms between their R structure and the T1 structure of Golovastikov.

Things become easier if one introduces another triple and pseudo-monoclinic unit cell of the G unit cell using the transformation matrix  $P = \begin{pmatrix} 2 & -1 & -1 \\ 1 & 1 & -1 \\ 1 & 1 & 0 \end{pmatrix}$  and centring translations  $0, 0, 0; 2/3, 1/3, 2/3; 1/3, 2/3, 1/3$ . The unit cell vectors are now located in the hexagonal and monoclinic planes. Moreover, this unit cell is a 9-fold multiple of a smaller pseudo-monoclinic unit cell  $\langle T \rangle$ , itself equivalent to a pseudo-monoclinic  $\langle M \rangle$  unit cell (Fig.1), similar to the one found for the monoclinic polymorphs M1 and M3. This model is referred to as  $9\langle T \rangle P\bar{1}$  in Table 1. The transformation matrix between the G and  $\langle M \rangle$  unit cell is given by  $P = \begin{pmatrix} 1 & 0 & 1 \\ -1 & 1 & 1 \\ 0 & -1 & 1 \end{pmatrix}$ . Below, models are labelled by combining the shape (and/or the multiplicity of the unit cell) and the space group used to generate the atomic positions.

Within the triclinic  $P\bar{1}$  symmetry, the two  $\langle T \rangle$  and  $\langle M \rangle$  average unit cells are “fully equivalent”, due to a conservation of the inversion centres. Within the monoclinic symmetry, a change of elementary block is related to a change of space group. Both so-called  $3\langle M \rangle Pc$  and  $3\langle T \rangle Pn$  models (Table 1) have been checked for polymorph M1, with very similar refinements, except for a characteristic superstructure Bragg

line which clearly favours the  $3\langle M \rangle$  Pc model with the  $\langle M \rangle$  monoclinic elementary block. As shown by Nishi et al. [4], the  $\langle M \rangle$  elementary block contains two rhombohedral unit cells.

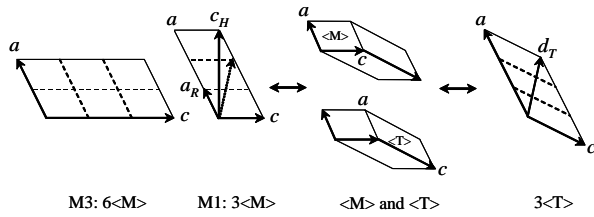


Fig. 1. Important directions and superstructure relationship in the monoclinic plane between the  $C_3S$  polymorphs discussed in the text. Tripling the unit cell along the  $b$  vector transforms  $3\langle T \rangle$  into  $9\langle T \rangle$ .

Table 1. Crystallographic data of various  $C_3S$  polymorphs.  $3\langle M \rangle$ ,  $3\langle T \rangle$ ,  $6\langle M \rangle$  and  $9\langle T \rangle$  are condensed notations for  $(3\mathbf{a}_{\langle M \rangle})$ ,  $(3\mathbf{a}_{\langle T \rangle})$ ,  $(2\mathbf{a}_{\langle M \rangle}, 3\mathbf{c}_{\langle M \rangle})$  and  $(3\mathbf{a}_{\langle T \rangle}, 3\mathbf{b}_{\langle T \rangle})$  supercells.

Polymorph	Shape	Space Group	a (Å)	b (Å)	c (Å)	$\alpha$	$\beta$	$\gamma$	V (Å <sup>3</sup> )	Authors
R		R3m	7.135	7.135	25.586	90	90	120	1128	Nishi et al. [3]
M3		Cm	33.083	7.027	18.499	90	94.12	90	4289	Nishi et al. [4]: choice 1
M3	$6\langle M \rangle$	Cm	33.0577	7.0330	18.5179	90	94.18	90	4294	our data: choice 1
		Im	18.5179(10)	7.0330(4)	36.694(19)	90	116.038(4)	90	4294	our data: choice 3
$\langle M \rangle$		Cm	12.235	7.073	9.298	90	116.31	90	721	Mumme [6]
$\langle M \rangle$		Am	9.259	7.0330	12.231	90	116.04	90	716	our data
M1	$3\langle M \rangle$	Pc	27.8736(2)	7.0590(5)	12.2575(8)	90	116.030(6)	90	2167	our data
M1	$3\langle T \rangle$	Pn	27.8736(8)	7.0601(8)	18.3439(2)	90	143.105(6)	90	2167	our data
T1(G)		$P\bar{1}$	11.67	14.24	13.72	105.50	94.33	90	2190	Golovastikov et al. [2]
T1	$9\langle T \rangle$	$P\bar{1}$	27.909(1)	21.123(1)	18.390(1)	90.390(2)	143.000(2)	89.630(2)	6524	our data
T1	$\langle T \rangle$	$P\bar{1}$	9.3037(5)	7.0411(4)	18.391(1)	90.388(3)	143.003(2)	89.637(3)	725	our data

Depending on the symmetry, the important directions of the structure, – relating to the axes of the monoclinic  $\langle M \rangle$  elementary block, – are the following:

Rhombohedral  $\mathbf{a}_R = \mathbf{a}_{\langle M \rangle}$ ,  $\mathbf{a}_H$ ,  $\mathbf{b}_H$ ,  $\mathbf{c}_H = \mathbf{c}_{\langle M \rangle} + 3\mathbf{a}_{\langle M \rangle}$

Monoclinic  $\mathbf{a}_{\langle M \rangle}$ ,  $\mathbf{b}_{\langle M \rangle} = \mathbf{a}_H + \mathbf{b}_H$ ,  $\mathbf{c}_{\langle M \rangle}$ ,  $2\mathbf{a}_H = \mathbf{b}_{\langle M \rangle} - \mathbf{c}_{\langle M \rangle}$ ,  $2\mathbf{b}_H = \mathbf{b}_{\langle M \rangle} + \mathbf{c}_{\langle M \rangle}$

Triclinic  $\mathbf{a}_{\langle T \rangle} = \mathbf{a}_{\langle M \rangle}$ ,  $\mathbf{b}_{\langle T \rangle} = \mathbf{b}_{\langle M \rangle}$ ,  $\mathbf{c}_{\langle T \rangle} = \mathbf{c}_{\langle M \rangle} - \mathbf{a}_{\langle M \rangle}$ ,  $\mathbf{b}_G = 2\mathbf{a}_H$ ,  $\mathbf{a}_G + \mathbf{c}_G = \mathbf{c}_{\langle T \rangle} + 3\mathbf{a}_{\langle T \rangle}$

One observes a conservation of the rhombohedral direction  $\mathbf{a}_R = \mathbf{a}_{\langle M \rangle}$  as a common repeat unit for all the  $C_3S$  polymorphs, with various superstructures. Passing from the rhombohedral to the monoclinic symmetry, the two hexagonal periodicities  $2\mathbf{a}_H$  and  $2\mathbf{b}_H$  are preserved as diagonals of the monoclinic unit cells, but the two hexagonal periodicities  $\mathbf{a}_H$  and  $\mathbf{b}_H$  are replaced by glide operations. The hexagonal periodicity  $\mathbf{c}_H$  appears as a diagonal of the unit cell of polymorph M1 but disappears in polymorph M3. The hexagonal base contains the

monoclinic cell vectors  $\mathbf{a}_{\langle M \rangle}$  and  $\mathbf{b}_{\langle M \rangle}$  and still represents an important plane of the structure. Going from the monoclinic symmetry to the triclinic one, the  $\mathbf{a}_{\langle M \rangle}$  and  $\mathbf{b}_{\langle M \rangle}$  directions are kept, but a superstructure appears. The  $\mathbf{c}_{\langle T \rangle}$  axis moves outside the hexagonal plane of the structure, but one hexagonal periodicity  $2\mathbf{a}_H$  is kept. The - common - diagonal of the triclinic unit cells,  $\mathbf{d}_T = \mathbf{a}_G + \mathbf{c}_G = \mathbf{c}_{\langle T \rangle} + 3\mathbf{a}_{\langle T \rangle}$ , - either the Golovastikov unit cell or ours, - now replaces the hexagonal  $\mathbf{c}_H$  periodicity.

### 3. Constant directions versus structural elements of the average structure $\langle M \rangle$

Averaging each structure, M3, M1 and T1, over its elementary block enables comparison, after dilatation and cell origin shifts, with the same final unit cell  $\langle M \rangle$  in which the atomic positions are very close to simple fractional positions.

The organisation of the structure as a 3-D packing of complex-shaped and distorted calcium polyhedra have been discussed by previous authors (Golovastikov et al. [2], Il'Inets et al. [5]). But this scheme does not lead to clear understanding, except for the high temperature R-polymorph within which there are three types of hexagonal sheets and a single type of calcium polyhedron per layer.

In fact, the same features also occur for the silicates. We reference the three silicate hexagonal layers as  $H_1$ ,  $H_2$ ,  $H_3$ , and the corresponding types of silicates as  $Si_1$ ,  $Si_2$ ,  $Si_3$ .

The  $Si_2$  and  $Si_3$  silicates are the first neighbours:  $d(Si_2-Si_3) \approx 4.8\text{\AA}$ . The  $Si_1$  silicates have more distant neighbours:  $d(Si_1-Si_{2,3}) \approx 5\text{\AA}$  for the first neighbours of the  $Si_1$  silicates.

The matter becomes clearer and more fruitful with the description of calcium and silicate skeleton in terms of 1-D and 2-D elements, among which the various chemical entities are distributed.

As in Fig. 2, one observes two types of atomic layers and three types of chains. The two families of alternate monoclinic layers are sketched in Fig 2a and 2b. The mixed layers (2a) contain silicates, calcium atoms and the isolated oxygen atoms.

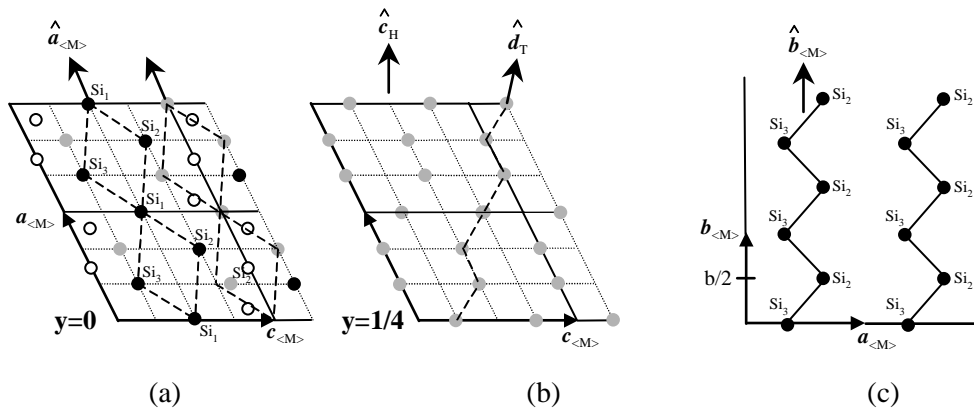


Fig.2. a, b: herringbone-like (a) and zigzag (b) chains in the monoclinic layers. ● Si ● Ca ○ O (isolated)  
 c: zigzag chains of silicates along the  $\mathbf{b}_{<M>}$  monoclinic axis.  
 The arrows  $\hat{\mathbf{a}}_{<M>}$ ,  $\hat{\mathbf{b}}_{<M>}$ ,  $\hat{\mathbf{c}}_H$  and  $\hat{\mathbf{d}}_T$  indicate directions.

The silicates of the mixed layers (Fig. 2a) form infinite herringbone-like chains propagating along the rhombohedral direction with the  $\text{Si}_1$  silicates at the crossing points. They are separated by similar calcium herringbone-like chains (also containing isolated oxygen atoms). The calcium atoms of the calcium-only layers (Fig. 2b) are arranged in infinite zigzag chains parallel to the  $\mathbf{d}_T$  direction of the diagonal of triclinic unit cells. The first silicate neighbours ( $\text{Si}_2$ ,  $\text{Si}_3$ ) also constitute infinite zigzag chains (Fig. 2c) parallel to the monoclinic  $\mathbf{b}_{<M>}$  direction. Two consecutive silicates in a zigzag chain belong to two adjacent  $H_2$  and  $H_3$  hexagonal sheets and to two distinct herringbone-like chains of the monoclinic layers.

Due to the 3-fold pseudo-symmetry, three families of chains, each of them (Fig. 2c) normal to the hexagonal axis, constitute a network of zigzag chains which itself constitutes a set of “thick” layers (two adjacent planes  $H_2+H_3$ ) containing all the first-neighbour silicates and only them. They are separated by the hexagonal planes  $H_1$  of silicates  $\text{Si}_1$ . Holes in the thick layers, forming an hexagonal network, are crossed by the oblique chains of calcium ions.

Looking at the orientational disorder, one finds that the disorder of the  $\text{Si}_2$  and  $\text{Si}_3$  silicates of the thick layers is rather simple with “gear-like” configurations, whereas the disorder of the  $\text{Si}_1$  silicates is more complex and frustrated in the high temperature polymorphs.

Going back to the discussing of the previous paragraphs, one can conclude that each of the important crystallographic directions  $\mathbf{a}_{\langle M \rangle}$ ,  $\mathbf{b}_{\langle M \rangle}$  and  $\mathbf{d}_T$ , discussed above corresponds to a 1-D structural element: zigzag or herringbone-like, calcium or silicate chain.

No 1-D structural element can be related to the hexagonal axis  $\mathbf{c}_H$ . However, 2-D structural elements, the  $H_1$  and  $H_2+H_3$  silicate layers, are found to be related to this direction. Note that the silicate triplets along this  $\mathbf{c}_H$  direction, discussed in the literature, are not relevant to the discussion of the orientational disorder, which is related to the first  $\text{Si}_2\text{-Si}_3$  neighbours.

#### 4. Discussion

Distribution of the chemical entities among 1-D and 2-D elements is obvious. The  $3\mathbf{a}_{\langle M \rangle}$  and/or  $3\mathbf{b}_{\langle M \rangle}$  superstructures found in T1 and M1 polymorphs of pure  $\text{C}_3\text{S}$  and sulphate-doped M1 polymorph are probably related to disorder or substitution in the silicate chains. On the other hand, the Mg-doped M3 polymorph exhibits a  $(2\mathbf{a}_{\langle M \rangle}, 3\mathbf{c}_{\langle M \rangle})$  superstructure. It is more likely related to a substitution of the calcium ions in calcium layers which allow a high degree of freedom due to the lower symmetry.

Tricalcium Silicate is very hard to grind, but evidence from optical examination and X-ray diffraction suggests the possibility of an easy cleavage along the hexagonal base. The hypothesis of a silicate skeleton driven cohesion is consistent with the existence of two types of hexagonal sheets: (hard?) “thick” layers of orientationally correlated first neighbour silicates separated by (soft?) “fuzzy” layers of frustrated silicates which are at greater distances from their first neighbours.

#### Conclusion

All the polymorphs can be described in terms of superstructures of two elementary blocks  $\langle M \rangle$  or  $\langle T \rangle$ . These elementary blocks become equivalent after averaging and origin translations.

The three constant directions shown by the metric analysis and the superstructure relationships between the polymorphs are related to 1-D and 2-D structural elements, and linked to the chemical distribution.

The distribution of the chemical entities between layers and between various types of chains is always related to the monoclinic pseudo-symmetry elements, whereas the anisotropy of the cohesive properties is related to the pseudo-hexagonal symmetry.

## References

- [1] Jeffery, J.W.: The Crystal Structure of Tricalcium Silicate. *Acta Crystallogr.* **5** (1952) 26-35.
- [2] Golovastikov, N.I.; Matveeva, R.G.; Belov, N.V.: Crystal Structure of the Tricalcium Silicate  $3\text{CaO}\cdot\text{SiO}_2 = \text{C}_3\text{S}$ . *Sov. Phys. Crystallogr.* **20**[4] (1975) 441-445.
- [3] Nishi, F.; Takeuchi, Y.: The Rhombohedral Structure of Tricalcium Silicate at  $1200^\circ\text{C}$ . *Z. Kristallogr.* **168** (1984) 197-212.
- [4] Nishi, F.; Takeuchi, Y.; Maki, I.: The Tricalcium silicate  $\text{Ca}_3\text{O}[\text{SiO}_4]$ : the monoclinic Superstructure. *Z. Kristallogr.* **172** (1985) 297-314.
- [5] Il'inets, A.M.; Malinovskii, Yu. A.; Nevskii, N.N.: Crystal structure of the rhombohedral modification of tricalcium silicate  $\text{Ca}_3\text{SiO}_5$ . *Sov. Phys. Dokl.* **30** (1985) 191.
- [6] Mumme, W.G.: Crystal Structure of Tricalcium Silicate from a Portland Cement Clinker and its Application to Quantitative XRD Analysis. *N. Jb. Miner. Mh.* **H. 4** (1995) 145-160.
- [7] Courtial, M.; de Noirfontaine, M.-N.; Dunstetter, F.; Gasecki, G.; Signes-Frehel, M.: Polymorphism of Tricalcium Silicate in Portland Cement: a fast visual identification of structure and superstructure. *Powder Diffr.* In Press (2002).
- [8] Rietveld, H.M.: A profile method for nuclear and magnetic structures, *J. Appl. Crystallogr.* **2** (1969) 65-71.
- [9] Rodriguez-Carvajal, J.: The Rietveld Method in Practice: the program FULLPROF, Note prepared for the Nordic Research Course (1994).